NUMERICAL STUDY ON SPONTANEOUS IGNITION OF PRESSURIZED HYDROGEN RELEASE THROUGH A TUBE

B.P. Xu, J.X. Wen and V.H.Y. Tam*
Centre for Fire and Explosion Studies, Faculty of Engineering, Kingston University
Friars Avenue, London, SW15 3DW, UK

* Correspondence: j .wen@kingston.ac.uk

ABSTRACT

The issue of spontaneous ignition of highly pressurized hydrogen release is of important safety concern, e.g. in the assessment of safety risk and design of safety measures. This paper reports on recent numerical investigation of this phenomenon through releases via a tube using a 5^{th}-order WENO scheme. A mixture-averaged multi-component approach was used for accurate calculation of molecular transport. The auto-ignition and combustion chemistry were accounted for using a 21-step kinetic scheme.

The numerical study revealed that the finite rupture process of the initial pressure boundary plays an important role in the spontaneous ignition. The rupture process induces significant turbulent mixing at the contact region via shock reflections and interactions. The predicted leading shock velocity inside the tube increases during the early stages of the release and then stabilizes at a constant value. The air behind the leading shock is shock-heated and mixes with the released hydrogen in the contact region. Ignition is firstly initiated inside the tube and then a partially premixed flame is developed. Significant amount of shock-heated air and well developed partially premixed flames are two major factors providing potential energy to overcome the strong under-expansion and flow divergence following spouting from the tube.

Further parametric studies were conducted to investigate the effect of rupture time, release pressure, tube length and diameter on the likelihood of spontaneous ignition. A slower rupture time and a lower release pressure will lead to increases in ignition delay time and hence reduces the likelihood of spontaneous ignition. If the tube length is smaller than a certain value, even though ignition could take place inside the tube, the flame is unlikely to be sufficiently strong to overcome under-expansion and flow divergence after spouting from the tube and hence is likely to be quenched.

Keywords: Hydrogen; Shock; Rupture time; Spontaneous ignition; Molecular transport; Release pressure

1. INTRODUCTION

As a next-generation energy carrier, the safe transport and utilization of hydrogen is important for its wide adoption. Owing to its lowest density among all gases, hydrogen is stored either at high pressure or as a liquid at low temperature. The subject of this paper is on the consequence of an accidental release of pressurized hydrogen.

A review of historic data showed that in some accidental scenarios, pressurized hydrogen releases were found to have ignited although there were no clearly identifiable ignition sources [1]. Among the postulated mechanisms of spontaneous ignition, diffusion ignition has been demonstrated in experiments, i.e. laboratory and full scale tests [2-5] as well as theoretical and numerical investigations [6-10].

Since Wolanski and Wojciki's pioneering work of diffusion ignition [3] nearly 40 years ago. little work was done until recent years coinciding with the surge of interest in hydrogen as a future energy carrier. Further experimental studies have been conducted to demonstrate diffusion ignition of pressurized hydrogen release through a tube almost simultaneous by Dryer et al. [2], Golub et al. [4] and Mogi et al. [5]. In all these tests, bursting disks were used to initially separate the pressurized hydrogen and air. Both Golub et al. and Mogi et al. found that the minimum release pressure required for spontaneous ignition to occur depends on the tube length. As the tube length increases, the

minimum release pressure required to trigger a spontaneous ignition was found to decrease. Dryer et al. [2] provided further insight revealing that the internal geometry downstream of the burst disk greatly affected the likelihood of spontaneous ignition, especially for relatively low release pressures. This led to the postulation that the bursting disk rupture process has an important influence on mixing and ignition through multi-dimensional shock formation, reflection and interactions.

When pressurized hydrogen is released into an ambient environment via a tube through fast rupturing of a pressure boundary, strong shock waves are generated inside the tube. The leading shock wave is driven into the ambient air and the temperature of the air behind the shock is elevated. The shock-heated air mixes with the released hydrogen at the contact region. Ignition might occur inside the tube first under specific conditions and then the initiated flame might also survive the high under-expansion while sprouting from the tube and transit to a turbulent jet fire. Dryer [2] estimated that the typical characteristic time scale in the release tube is less than 100 μs and the mixing at the contact region is a limiting factor for the ignition. Related experiments for similar flow conditions [11-13] indicated that there exists substantial turbulent mixing at the contact region inside the tube. Although the mechanism of the actual turbulent mixing process is still not well understood, it has been found that the rupturing process, which generates strong multi-dimensional shock waves, plays an important role in the mixing [11-13].

The present study uses a fully compressive Navier Stokes solver with real physical viscosity and a 5^{th} order WENO scheme to gain insight of the spontaneous ignition mechanism in pressurized hydrogen release via a tube. We attempt to shed light on the following questions: what is the mechanism of the turbulent mixing at the contact region? Where and when would ignition take place? If ignition occurs inside the tube, how could the initiated flame survive the high under-expansion region, as the release flow is sprouting out of the tube exit? What are the key factors affecting the ignition occurrence? Finally, what is the possible mechanism to start a final turbulent jet fire observed by experiments [2,4]?

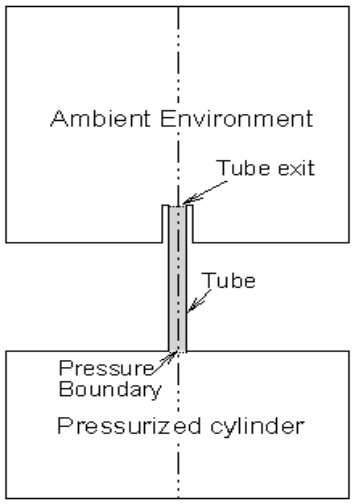

Figure 1. Schematic of the computational domain.

2. NUMERICAL METHODS

Molecular diffusion across the contact region is a much slower process than the fast characteristic flow time. To calculate physical diffusion at the contact surface, high order numerical schemes along with fine grid resolution are required to keep numerical diffusion under control. For applications involving rich shock structures, high-order weighted essentially non-oscillatory (WENO) shock-capturing schemes are more efficient than low order total variation diminishing (TVD) schemes and produce lower numerical diffusion [14].

Exploiting the symmetric nature of the problem and the limitation of current computing resources, two-dimensional simulations were conducted. The numerical schemes are based on an arbitrary Lagrangian and Eulerian (ALE) method [15] in which convective terms are solved separately from the other terms. Each time cycle is divided into two phases: a Lagrangian phase and a rezone phase. Considering the substantial scale difference between diffusion and advection, different numerical

schemes were adopted in the two phases. In the Lagrangian phase, a second-order Crank-Nicolson scheme is used for the diffusion terms and the terms associated with pressure wave propagation, a 3rd - order TVD Runge-Kutta method [16] is used in the rezone phase to solve the convective terms. The coupled semi-implicit equations in the Lagrangian phase are solved by a SIMPLE type algorithm with individual equations solved by a conjugate residual method [17]. For spatial differencing, a 5th-order upwind WENO scheme [16] is used for the convection terms and the second-order central differencing scheme is used for all the other terms.

A mixture-averaged multi-component approach [18] was used for the calculation of molecular transport with consideration of thermal diffusion which is important for non-premixed hydrogen combustion. For autoignition chemistry, Saxena and Williams' detailed chemistry scheme [19] which involves 21 elementary steps among 8 reactive chemical species was used. The scheme was previously validated against a wide range of pressures up to 33 bar. It also gave due consideration to third body reactions and the reaction-rate pressure dependent "falloff" behavior. Since high-pressure hydrogen release undergoes strong under-expansion after discharging into an open space, a detailed chemistry allowing for the pressure dependant reaction rate is essential to accurately predict chemical reaction rates. To deal with the stiffness problem of the chemistry, the chemical kinetics equations were solved by a variable-coefficient ODE solver [20].

Table 1 Computational details

Parameters	**Values**
Rupture time (μs)	5, 10, 25
Release pressure (bar)	50, 100, 150
Initial Temperature (K)	293
Diameter of tube (mm)	3, 6
Length of tube (mm)	30, 60, 100
Thickness of film(mm)	0.1
Minimum grid spacing (μm)	15

3. PROBLEM DESCRIPTIONS

The schematic plot of the computational domain shown in Fig. 1 is composed of three cylindrical regions: pressurized cylinder, a release tube and ambient environment. To resolve the large scale vortices existing around the tube exit, the tube is inserted into the ambient environment 8mm from the top. The distance of 8mm was so chosen that the leading spherical shock would not be reflected back from the bottom wall of the ambient region to interfere with the formation of the vortices during the simulations. As discussed, the rupture process of the initial pressure boundary is essential to the spontaneous ignition. The Iris model [21] is used to simulate the finite opening time of the pressure boundary. It assumes the pressure boundary, which is mimicked by a thin diaphragm with a thickness of 0.1 mm placed at the bottom plane of the release tube in the simulations, ruptures linearly from the centre at a finite pre-determined rate as simulations start.

a) Logarithm of pressure (bar) (b) Axial velocity (m/s)

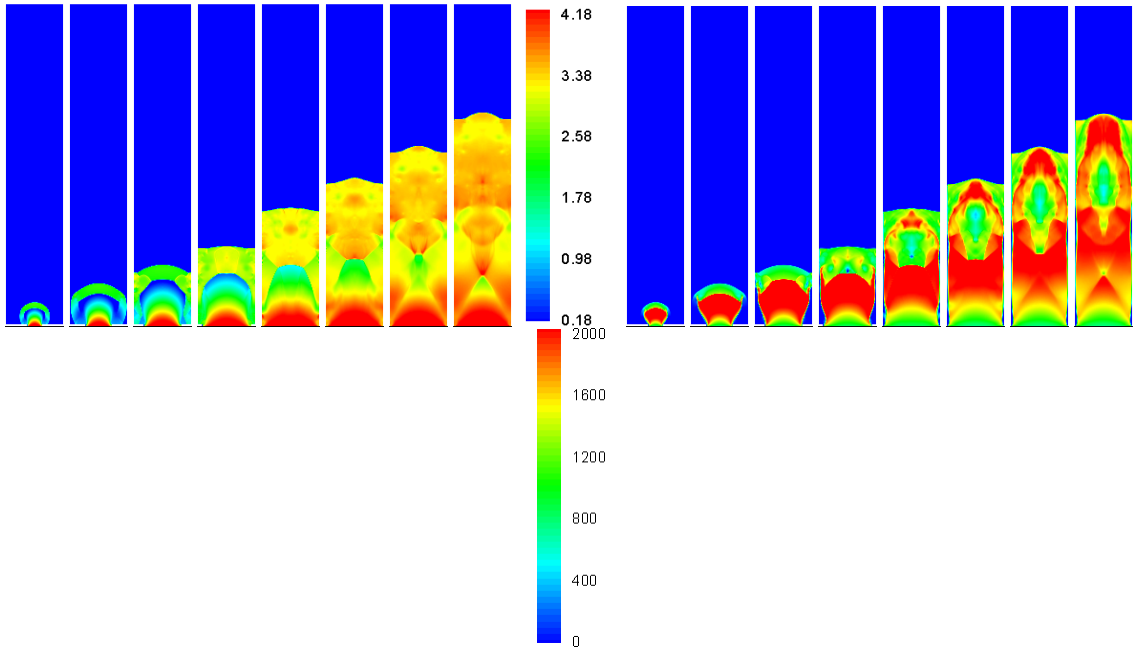

Figure 2. Predicted contours of pressure and axial velocity for a 150 bar release with a rupture time of 5 µs at a time interval of 1 µs.

All the simulations were started from still conditions with the tube and ambient environment regions filled with ambient air and the pressurized cylinder region with pure pressurized hydrogen separated by a thin diaphragm. All the solid surfaces (e.g. walls) were assumed to be non-slip and adiabatic. Non-uniform grids were applied to the regions of pressurized cylinder and ambient environment and uniform grids to the tube region. Since flame is initiated at the thin contact region, a very fine grid resolution is required there to resolve the species profiles in the ignited flame [22]. In this case, a 15 µm mesh size is adopted to resolve the contact region, which is also close to the grid resolution of 20 µm in [7,22]. The pressurized cylinder was set up to be sufficiently large to ensure that the pressure drop during the simulation does not exceed 3% of the initial pressure. The key parameters of the computed release scenarios are listed in Table 1. The rupture time in table 1 is the time to full bore opening of the thin diaphragm.

4. RESULTS AND ANALYSIS

4.1 Release flow inside the tube

a) Logarithm of pressure (bar) (b) Axial velocity (m/s)

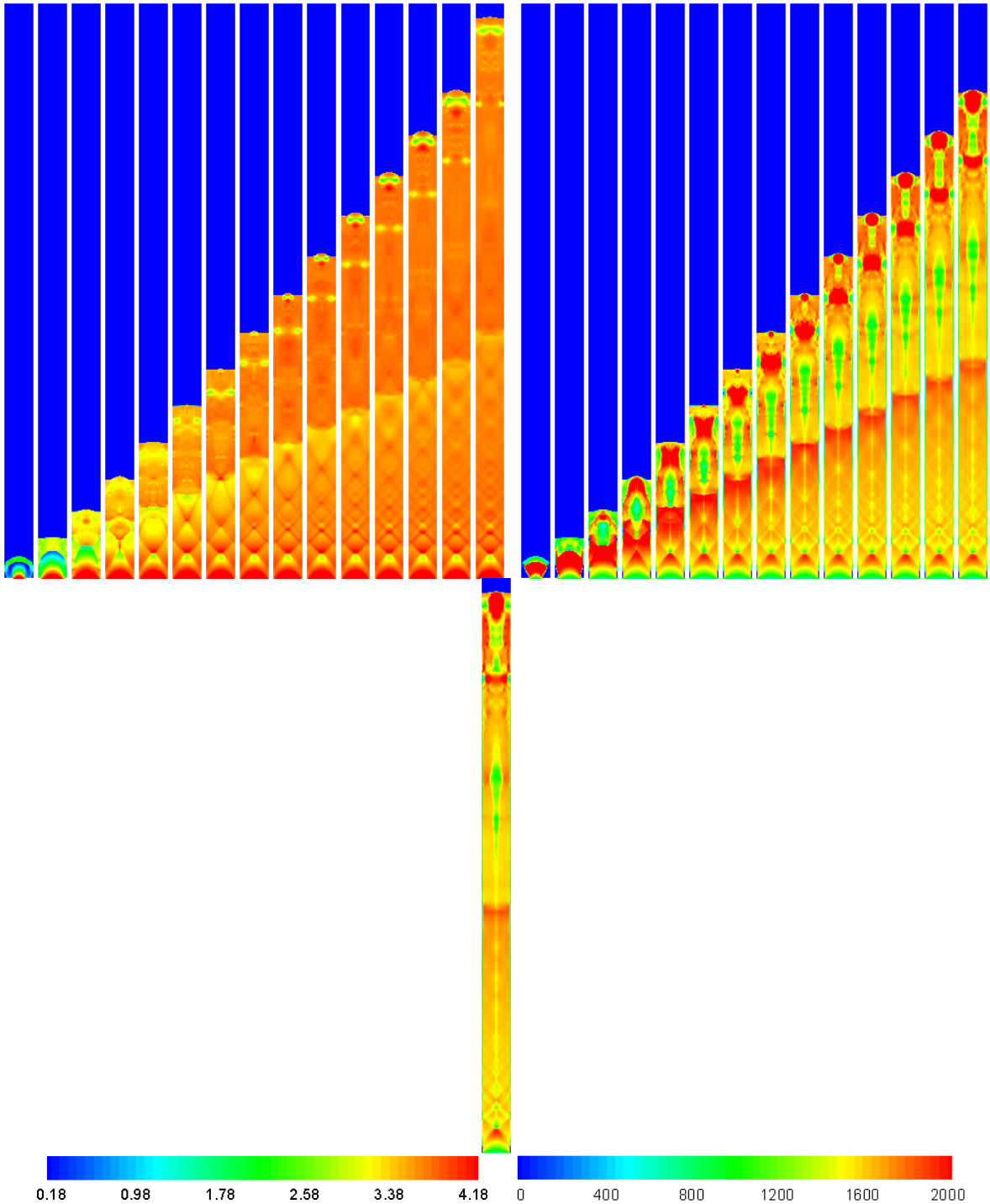

Figure 3. Predicted contours of pressure and axial velocity for a release case of 150bar and a rupture time of 5 μs at a time interval of 2 μs.

The actual rupture process of the rupturing disk or diaphragm has a finite rate and plays an important role in the flow development inside the tube. If a planar pressure boundary is assumed to rupture instantaneously and the effect of boundary layer is neglected, the release can be treated as one-dimensional flow inside the tube. Previous studies [23, 24] revealed that this treatment would incur errors especially at early stage of the release and the finite rupture time has to be considered.

Fig. 2 shows the predicted contours of pressure and axial velocity for a release case of 150 bar and a rupture time of 5 μs during early stages of the release. Following the rupture, an under-expanded hydrogen jet firstly appears. A leading curvilinear shock is quickly generated at the front of the jet and a Mach shock gradually arises inside the expanded hydrogen. As the leading shock reaches the tube wall, it is reflected as transverse shock waves which converge at the axial line and then move towards

the wall again. This process can repeat several times inside the tube and gradually dissipate away from the location of the initial pressure boundary. Ahead of the Mach shock, the flow velocity quickly decelerates and the pressure is recovered. As the jet touches the wall, a high speed annular flow develops near the wall and touches again to form a central flow at the axial line downstream. A high speed region emerges behind the leading shock. Similar to the mechanism of formation of the Mach shock, another shock arises at the front of the high speed region. This process repeats itself inside the tube and an intermittent flow pattern of circular and central flows is formed.

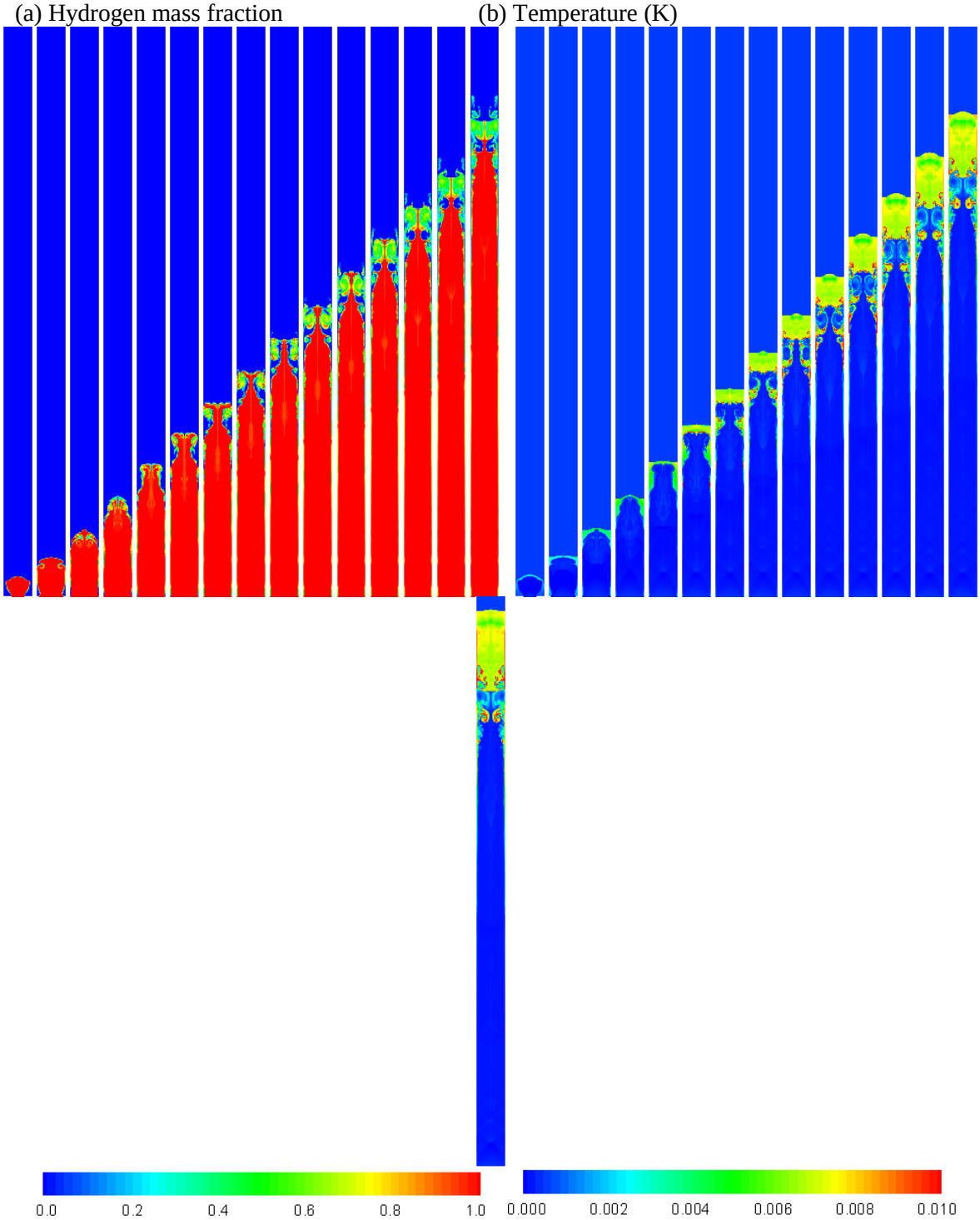

Figure 4. Predicted contours of hydrogen mass fraction and temperature for a 150 bar release with a rupture time of 5 µs at a time interval of 2 µs.

Owing to the aforementioned two processes, i.e. reflections and interactions of shock waves and the formation of the intermittent flow pattern, the release flow inside the tube is highly turbulent and the contact region is highly distorted by the flow development. As the transverse shocks sweep through the contact region, the misalignment of the pressure and density gradients causes a deposition of vorticity through the baroclinic production mechanism and would produce turbulent mixing via Rayleigh-Taylor instability. However, owing to the short characteristic time scale of the release, it is likely that the large scale turbulent flow is responsible for the substantial turbulent mixing at the contact region instead of Rayleigh-Taylor instability.

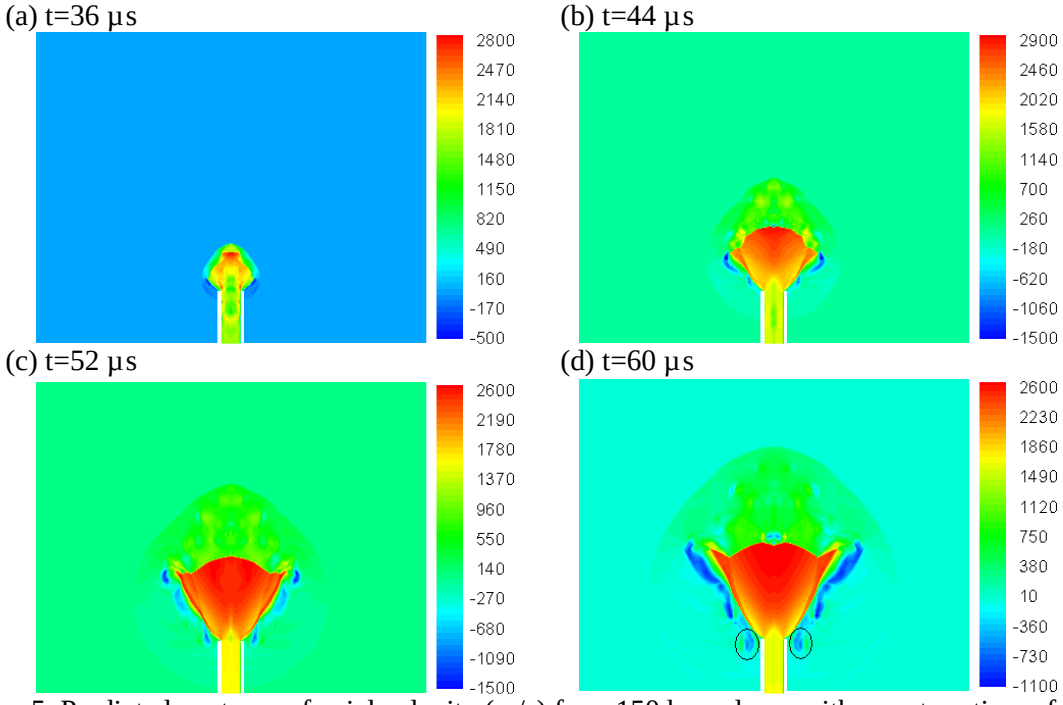

Figure 5. Predicted contours of axial velocity (m/s) for a 150 bar release with a rupture time of 5 µs at a time interval of 8 µs.

More predicted contour results are shown in Figs. 3-4 at a time interval of 2µs. The initially curvilinear shock quickly becomes planar due to the reflections of the transverse shocks. The aforementioned repeated intermittent flow pattern is more evident in the contour plots of axial velocity (Fig. 3b). The contact region is highly disturbed. Significant amount of flammable mixture is formed due to turbulent mixing (Fig. 4a). The air behind the shock is shock-heated, while hydrogen is cooled due to flow acceleration. The shock-heated air mixes with the cooled hydrogen to form a flammable mixture. If the temperature of the flammable mixture exceeds the hydrogen autoignition temperature, ignition would be initiated following an initial delay. A thin diffusion flame is observed after t=10µs in Fig. 4b. With the formation of significant amount of flammable hydrogen mixture due to increasing turbulent mixing, the flame starts to extend in the radial direction and gradually a partially premixed flame is formed. A very high temperature region is also found at the boundary mixing layer due to the relatively low heat dissipation rate.

(a) t=36 µs (b) t=44 µs

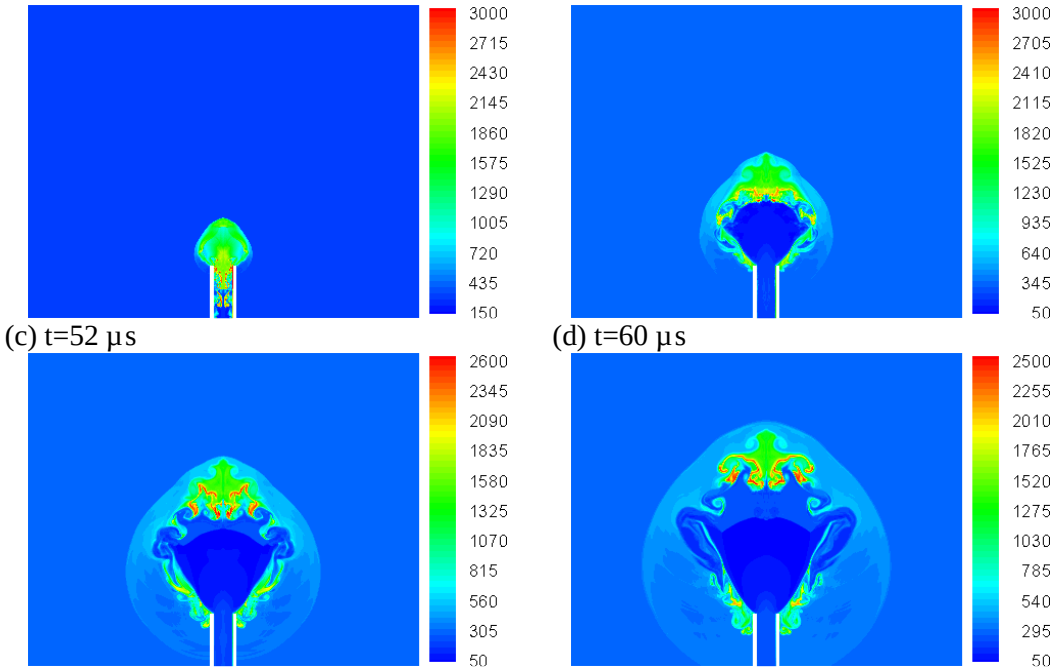

Figure 6. Predicted contours of temperature (K) for a 150 bar release case with a rupture time of 5 µs at a time interval of 8 µs.

4.2 Release into an open ambient environment

Fig. 5-6 show the contours of hydrogen axial velocity and temperature for a 150 bar release case through a 6 cm long tube respectively. The disk rupture time was 5 µs and the results were plotted at a time interval of 8 µs after the leading shock sprouts from the tube. Following exiting from the tube, a strong under-expanded jet is generated. The leading shock quickly loses its planar shape and turns into a dissipative spherical shock. At the early stage of the under-expansion, another important shock, called Mach shock, firstly arises in the shock-heated air in this case as significant amount of shock-heated air exists behind the leading shock. The Mach shock firstly emerges close to the tube exit edge due to strong diffraction waves originating from the edge and gradually integrates into a final Mach disk situating inside the expanded hydrogen. The diffraction waves are reflected back as compression waves by the lateral flow boundary and the coalescence of these compression waves results in a barrel shock structure encompassing the under-expanded region within the Mach shock. Outside the under-expanded region, the flow is decelerated and gas temperature and pressure are restored; while inside the region, the flow is accelerated and gas temperature drops. As the flame propagates through the under-expansion zone, its chemical reaction rates decrease and the flame has a tendency to be quenched due to heat loss from the expansion. Once the flame emerges out of the under-expansion zone, the reaction rates start to recover and re-ignition occurs in some cases at particular locations due to the high temperature of the shock waves. At t=44 µs, the recovered flame almost encompasses the whole under-expansion zone while the flame front has a higher temperature and will propagate further downstream. During the early stages of the release, a reverse flow develops at the lateral flow boundary (see Fig. 5), which brings the lateral flame back towards the tube exit merging with the flame there. There also exist large scale vortices (circled in Fig. 5d) around the exit, which induce a recirculation zone where a seed flame can be stabilized.

The aforementioned findings of the enclosed flame and the seed flame at the recirculation zone were also experimentally observed by Mogi et al. [4]. With the current grid resolution, the time step is in the order of 10^{-9} s, while the evolution time to obtain a jet fire is longer than 10^{-3} s according to the experimental measurement of Mogi et al. The simulations were hence not extended to cover the transition to jet fires due to limitation of the current computing resources. However, the findings from the present simulations suggest that there are two possible mechanisms which can lead to the transition to jet fire: (1) via the flame front propagating downstream; and (2) the seed flame stabilizing around the tube exit. The experimental observations of Mogi et al. suggested that the flame front would be

blown out by the flow development downstream and the seed flame might be responsible for the final turbulent jet fire. During their tests, no jet fire was observed in the absence of the seed flame.

4.3 Influencing factors of spontaneous ignition

Experimental studies [2, 4-5] have revealed that the release pressure and dimensions of tube are major influencing factors concerning the likelihood of spontaneous ignition. In this section, we present numerical investigations of these factors as well as the effect of finite rupture time of the rupturing disk. As ignition firstly occurs inside the tube, analysis is hence focused on the in-tube flow processes. Overall 7 test cases were numerically investigated and the key parameters are listed in Table 2.

Table 2 Key parameters of the test cases for investigating the influencing factors on spontaneous ignition

Cases	**1**	**2**	**3**	**4**	**5**	**6**	**7**
Release pressure (bar)	150	150	150	150	50	100	150
Rupture time (μs)	5	10	25	5	5	5	5
Diameter of tube (mm)	3	3	3	6	3	3	3
Length of tube (cm)	6	10	10	10	10	10	3
Ignition time (μs)	9	15	32	16	45	12	9

4.3.1 Effect of rupture time

Cases 1 to 3 were computed to investigate the effect of rupture time and results are shown in Fig.7. As we know from the above discussion, a curvilinear leading shock is firstly formed during the rupture process and then it quickly turns into a flat shock due to the reflections of transverse shock waves. After the release, the strength of the leading shock (judging from the shock velocity in Fig. 8a) gradually increases to a maximum and then slowly decreases. Although the shock velocity finally stabilizes at approximately the same value of around 2000m/s for the different rupture times, the longer the rupture time, the slower is the increase rate of the shock velocity.

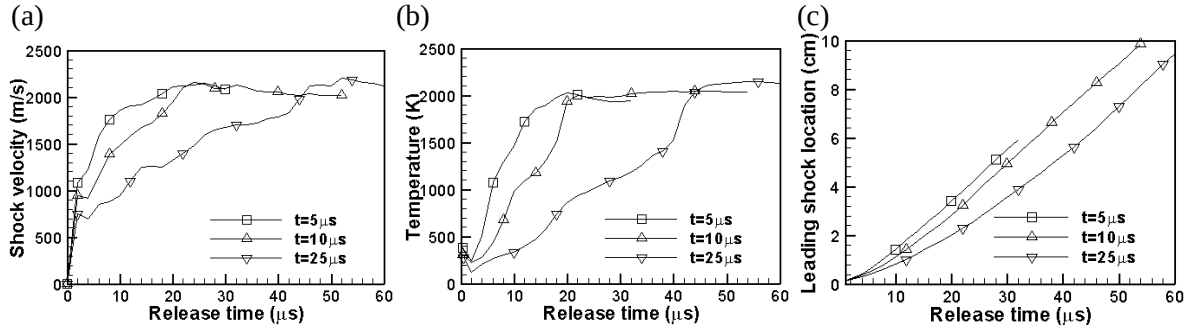

Figure 7. The effect of rupture time on spontaneous ignition, (a) the predicted leading shock velocity; (b) the volume averaged shock-heated air temperature; and (c) the leading shock location versus release time.

Owing to the non-uniform distribution of the shock-heated air temperature, volume averaged temperature were calculated and plotted in Fig. 7b. Because the shock-heated temperature is closely related to the leading shock strength, i.e. the shock velocity, the changing patterns of the volume averaged temperature closely resemble that of the shock velocity. Although the final volume averaged temperatures are approximately the same for all three cases, a slow rupture time would lead to slower increasing rate of the temperature and hence longer ignition delay time as listed in Table 2. In all three cases, the final volume averaged temperature is around 2000K. Fig. 7c shows the locations of the leading shock versus release time. For a fixed tube length, the flow time inside the tube is longer for a slow rupture time. As the rupture time increases from 5 μs to 25 μs, the ignition delay time increases from 9 μs to 32 μs. From Fig. 7c, it can be derived that the minimum required lengths for ignition to take place inside the tube are approximately 1.5cm and 4cm for rupture times of 5 μs and 25 μs, respectively. Therefore, a slow rupture time has an adverse effect on spontaneous ignition. We believe

that this was the main reason of the lower spontaneous ignition likelihood for releases through a short tube in the experiments of Dryer et al.[2], Mogi et al. [4] and Golub et al. [5].

4.3.2 Effect of tube diameter

The effect of tube diameters was investigated in Case 1 and 4 with two different tube diameters 3 and 6 mm. The predictions are shown in Fig. 8. In this study, it is assumed that the same opening speed is applied to different tube diameters. This would lead to a longer rupture time for large tubes. Owing to the longer rupture time, the increase rates of shock velocity and shock-heated temperature are slower for case 4 which has a larger tube diameter. However, the stabilized shock-heated temperature shows little dependence on the tube diameter. It can be seen from Table 2 that the ignition delay time increased to 16μs for Case 4 in comparison with 9μs for Case 1. From Fig. 8c, it can be derived that the minimum required length for ignition to take place is increased to 2cm for Case 4. This demonstrates that a large tube diameter can reduce the likelihood of spontaneous ignition. This is consistent with the experimental findings of Mogi et al. [4].

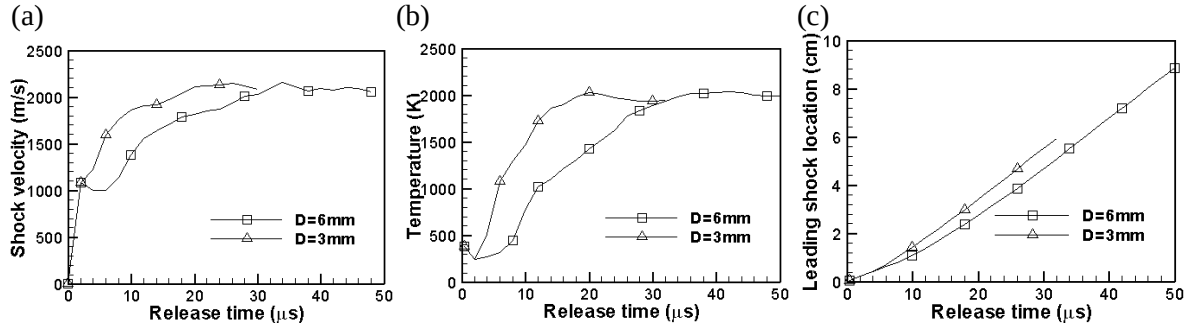

Figure 8. The effect of tube diameter on spontaneous ignition, (a) the predicted leading shock velocity; (b) the volume averaged shock-heated air temperature; and (c) the leading shock location versus release time.

4.3.3 Effect of release pressure

Case 1, 5 and 6 were computed to investigate the effect of release pressure. The rupture time was fixed at t = 5 μs for all the three cases. It can be seen in Fig. 9 that the shock-heated air temperature is strongly dependent on the release pressure. For the 50 bar release in Case 5, the maximum volume averaged temperature was predicted to be 1260 K and the ignition delay time 45 μs. Ignition was predicted at the boundary layer which is prone to ignition due to the relatively low velocity. Owing to the low momentum at the boundary layer, air tends to accumulate there and mixes with hydrogen from the main flow resulting in high flame temperature close to the wall. Even though the local flame temperature is high, it still cannot survive the expansion due to the strong diffraction waves originating from the tube exit edge. This demonstrates that although the flame at the boundary layer might facilitate the formation of the flame stabilizing around the exit, this alone is unlikely to produce the seed flame that would transit to a jet fire.

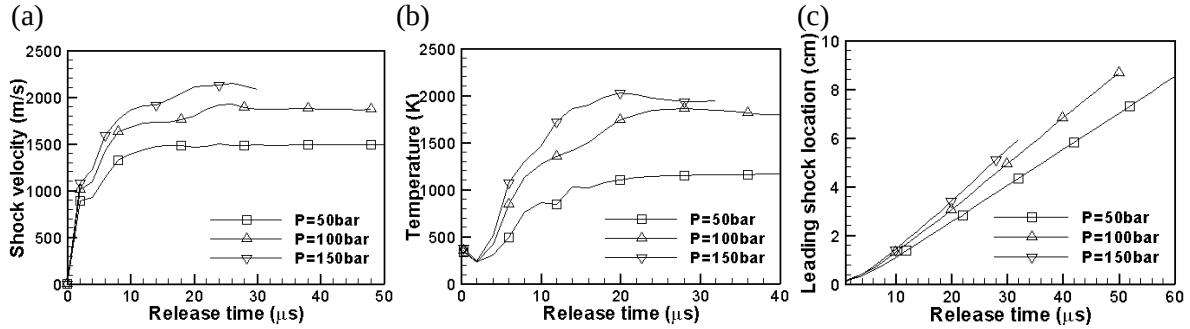

Figure 9. The effect of release pressure on spontaneous ignition, (a) the predicted leading shock velocity; (b) the volume averaged shock-heated air temperature; and (c) the leading shock location versus release time.

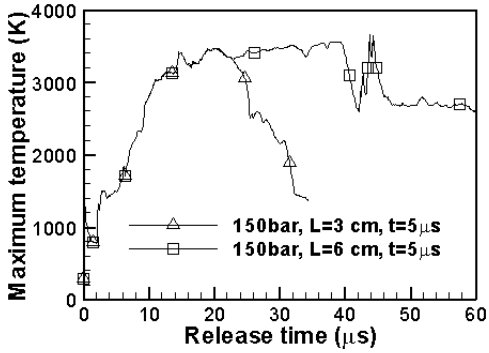

Figure 10. Maximum temperature versus release time for the cases with different tube lengths.

4.3.4 Effect of tube length

Case 1 and 7 with different tube lengths were simulated to investigate the effect of tube length. Fig. 10 shows the predicted maximum temperature versus release time. Since the only difference between the two cases is the length of the tube, ignitions occur after a delay time of 9 μs for both cases. Before the flames inside the short tube propagate into the under-expansion zone, the maximum temperature is exactly the same for both cases. Following spouting, the flame from the long tube survived the strong under-expansion, while the flame from the short tube was quenched. As shown in Fig. 4, inside the tubes, the major differences between the two cases are wider flame front (due to longer mixing time) and more shock-heated air ahead of the contact region (due to leading shock moving away from the contact region) for the case with a longer tube. The quenching process is illustrated in Fig. 11 by comparison of temperature contours scaled to the same value for both cases at three different moments after the leading shocks leaving the tube exits. In the case of the longer tube, there is more shock-heated air ahead of the flames in the contact region, the Mach shock is firstly generated inside the shock-heated air and ahead of the shock the air temperature recovered to a relatively higher value. As the flame penetrates the under-expansion zone and mixes with the high temperature air, it has more

potential energy to overcome further flow divergence. Furthermore, owing to the well developed partially premixed flame inside the tube, the flames from the longer tube prior to leaving the tube end were encompassed by a high temperature mixture. This would also facilitate the flame to survive the under-expansion and further flow divergence. For the case of the short tube, the Mach shock is firstly formed inside the cooler hydrogen, the temperature of the shock-heated air drops more quickly and the heat release from the chemical reactions can not compensate the heat loss due to flow divergence, resulting in the flame being quenched. In addition, the partially premixed flame in the short tube was not well developed due to the shorter mixing time and hence was less strong to overcome quenching effect of the under-expansion and flow divergence.

These results demonstrate that a longer tube not only provides longer mixing time to facilitate ignition to happen inside the tube, but also provides larger amount of shock-heated air and well developed partially premixed flames to survive the strong under-expansion and further flow divergence. Moreover, it suggests that if the tube length is smaller than a certain value, even though ignition may take place inside the tube, the flame will be quenched after spouting from the tube exit. This latter phenomena was also experimentally observed by Mogi et al. [4].

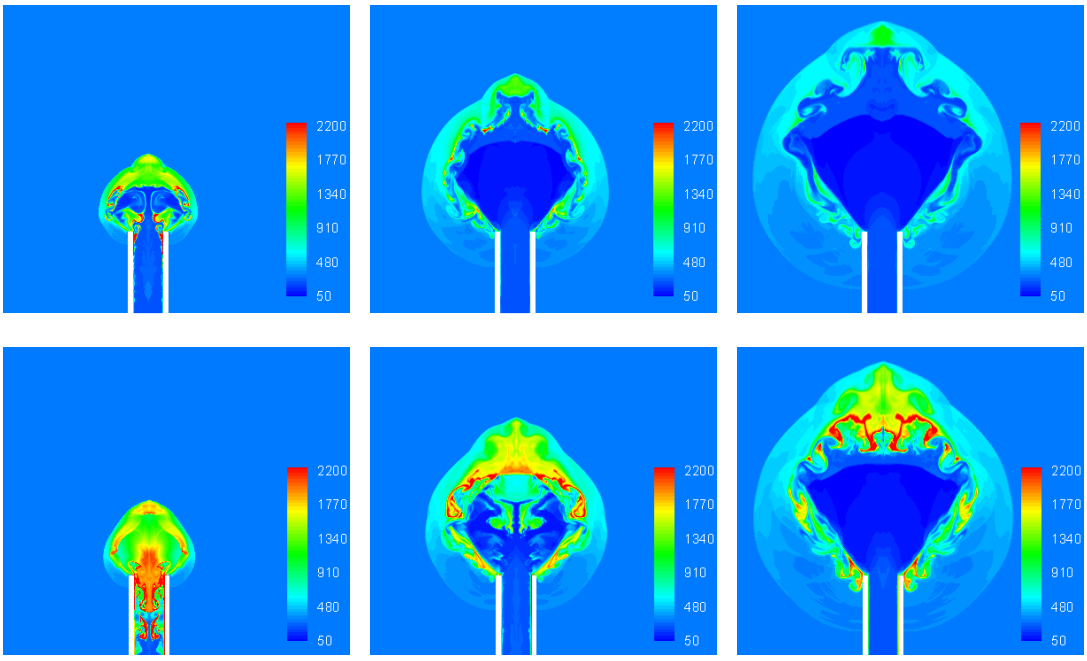

Figure 11. Comparison of temperature (K) contours for the cases of 3cm long tube (top row) and 6cm long tube (bottom row) at 4 µs, 10 µs, 16 µs afterspouting from the tube.

5. CONCLUSIONS

Numerical investigations have been carried out for pressurized hydrogen releases via a tube into ambient air. The predictions successfully captured the spontaneous ignition phenomenon experimentally observed by previous investigators [2,4-5] and offered further insight that were uncovered in previous experiments. The main findings can be summarized as follows:

The rupture process of the initial pressure boundary, which mimics the rupturing disk/diaphragm in experiments and in practice this corresponds to equipment rupturing times, plays an important role in the occurrence of spontaneous ignition. The rupture process produces reflected shock waves and intermittent flow development which induce significant turbulent mixing in the contact region. The velocity of the leading shock increases during the early stages of the release and then stabilizes at a constant value which is higher than that predicted in one-dimensional analysis. The air behind the leading shock is shock-heated and mixes with hydrogen in the contact region to form a significant amount of flammable mixture due to the enhanced turbulent mixing. Ignition is firstly initiated inside the tube. With the development of turbulent mixing a partially premixed flame evolves. Significant amount of shock-heated air and well developed partially premixed flames are two major factors providing potential energy to overcome the strong under-expansion and further flow divergence following spouting from the tube. The predictions show that the initial flames can survive at two

locations: (1) at the front of the under-expanded jet; and (2) within a recirculation zone near the tube exit. The latter is most likely to transit to a jet fire. A thin high temperature boundary layer flame is also found adjacent to the wall, which facilitates the formation of the flame around the tube exit.

Further parametric studies have shown that the rupture time, release pressure, tube length and diameter are major factors affecting the likelihood of spontaneous ignition. A slow rupture time significantly increases the ignition delay time due to the slow increasing rate of the leading shock velocity during the early stages of the release, and hence reduces the likelihood of spontaneous ignition. A decrease in release pressure greatly reduces the maximum shock-heated air temperature and therefore increases ignition delay time. If the ignition delay time is longer than the flow residence time inside the tube, no ignition would take place.

Following on from the above, it was further found that a longer tube not only provides a longer mixing time to facilitate ignition, but also provides larger amount of shock-heated air and well developed partially premixed flames to survive the strong under-expansion and further flow divergence. If the tube length is smaller than a certain value, even though spontaneous ignition may take place inside the tube, it is likely to be quenched following spouting. Release from a larger diameter tube is less prone to spontaneous ignition due to longer rupture time.

The present study suggests that the likelihood of spontaneous ignition can be mitigated by using a slow rupturing diaphragm and reducing the tube length to diameter (L/D) ratio.

REFERENCES

1. Astbury, G.R. and Hawksworth, S.J., Spontaneous ignition of hydrogen leaks: a review of postulated mechanisms, Int. J Hydrogen Energy, 32, 2007, pp. 2178-2185.
2. Dryer, F.L., Chaos, M, Zhao Z. Stein, J.N., Alpert, J.Y. and Homer. C.J., Spontaneous Ignition of Pressurized Releases of Hydrogen and Natural Gas into Air, Combust. Sci. and Tech., 179, 2007, pp. 663-694.
3. Wolanski, P. and Wojcicki, S., Investigation into the Mechanism of the Diffusion Ignition of a Combustible Gas Flowing into an Oxidizing Atmosphere. Proc. Combust. Instit., 14, 1972, pp. 1217-1223.
4. Mogi, T, Kim, D, Shiina, H and Horiguchi, S., Self-ignition and explosion during discharge of high-pressure hydrogen, Journal of Loss Prevention in the Process Industries, 21(2), 2008, pp. 199-204.
5. Golub, V.V. , Baklanov, D.I. , Bazhenova, T.V. , Bragin, M.V. , Golovastov, S.V., Ivanov, M.F. , Volodin, V.V., Shock-induced ignition of hydrogen gas during accidental or technical opening of high-pressure tanks, Journal of Loss Prevention in the Process Industries, 21(2), 2008, pp. 185-198.
6. Liu, Y.F., Sato, H., Tsuboi, N., Hjigashino, F., and Hayashi, A.K., Numerical simulation on hydrogen fuel jetting from high pressure tank. Sci. Tech. Energ. Mater., 67, 2006, pp. 7-11.
7. Yamada, E, Watanabe, S, Hayashi, A.K. and Tsuboi, N, Numerical analysis on autoignition of a high-pressure hydrogen jet spouting from a tube, Proc. Combust. Inst., 32(2), 2009, pp. 2363-2369.
8. Xu, B.P., Wen, J.X., Dembele, S., Tam, V.H.Y, Hawksworth, S.J., The effect of pressure boundary rupture rate on spontaneous ignition of pressurized hydrogen release, Journal of Loss Prevention in the Process Industries, 22(3), 2009, pp. 279-287.
9. Xu, B.P., Hima, L.EL, Wen, J.X., Dembele, S., Tam, V.H.Y, Donchev, T., Numerical Study of Spontaneous Ignition of Pressurized Hydrogen Release through a tube into Air, Journal of Loss Prevention in the Process Industries, 21(2), 2008, pp. 205 221.
10. B. P. Xu, L. EL Hima, J. X. Wen and V.H.Y. Tam, Numerical study of spontaneous ignition of pressurized hydrogen release into air, Int. J Hydrogen Energy, 2009, in press.
11. Vasil`eva, R.V., Turbulent mixing of driver and driven gases in a shock tube channel, Journal of applied mechanics and technical physics, 26(2), 1985.
12. Levine, M. A., Turbulent mixing at contact surface in a driven shock wave, Phys. Fluids, 13(5), 1970.
13. White, D.R., Influence of diaphragm opening time on shock flows, J. Fluid Mech., 4(6), 1958.
14. Jang, G.S. and Shu, C.W., Efficient Implementation of Weighted ENO Schemes, J. of Comput. Phys. 126, 1996, pp. 202-228.

15. C.W.Hirt, A.A.Amsden, J.L.Cook, J. Comput. Phys. 14 (1974) 227.
16. Balsara, D., Shu, C.W, Monotonicity Preserving Weighted Essentially non-oscillatory Schemes with Increasingly High Order of Accuracy, J. of Comput. Phys. 160, 2000, pp. 405-452.
17. P.J. O'Rourke, A.A. Amsden, Implementation of a conjugate residual iteration in the KIVA computer program, Los Alamos National Laboratory report LA-10849-MS, 1986.
18. R.J. Kee, F.A. Rupley, J.A. Miller, Chemkin II: a fortran chemical kinetics package for the analysis of gas-phase chemical kinetics. Sandia National Laboratories Report No. SAND89-8009, 1989.
19. Saxena, P. and Williams, F.A., Testing a small detailed chemical-kinetic mechanism for the combustion of hydrogen and carbon monoxide, Combustion and Flame, 145, 2006, pp. 316-323.
20. Brown, P.N., Byrne, G.D., Hinkmarsh, A.C., VODE, a variable-coefficient ODE solver, SIAM J. Sci. Stat. Comput. 10, 1989, pp.1038-1051.
21. Goozee, R.J., Jacobs, P.A., Buttsworth, D.R., Simulation of a complete reflected shock tunnel showing a vortex mechanism for flow contamination, Shock waves, 15(3-4), 2006, pp. 165-176.
22. Hilbert, R. and Thevenin, D., Autoignition of turbulent non-premixed flames investigated using direct numerical simulations, Combust. Flame 128, 2002, pp. 22-37.
23. Shtemenko, L.S., Shock-waves formation in shock-tube during the bursting of diaphragm, Vestnik Moskovskogo Universiteta Seriya 3 Fizika Astronomiya, 23(3), 1982, pp. 27-34.
24. Petrie, P. J. and Jacobs, P. A., Numerical simulation of diaphragm rupture, 20th International Symposium on Shock Waves, 1995.